The Gamma-Rays from Negative μ-Meson Capture in Lead*†

GERARD G. HARRIS‡ AND T. J. B. SHANLEY§
Palmer Physical Laboratory, Princeton University, Princeton, New Jersey
(Received November 6, 1952)

The gamma-rays produced when a negative μ-meson stops in lead have been studied by means of a cloud chamber in a magnetic field. The presence of these gamma-rays is confirmed. It is concluded that both nuclear gamma-rays and Bohr orbit gamma-rays are necessary to explain the experimental data.

INTRODUCTION

IT is known that when a negative μ-meson is captured by a nucleus only a small fraction of the meson-rest mass appears as nuclear excitation.[1,2] It is also known that the meson-rest-mass energy is not emitted in the form of energetic gamma-rays.[3–5] There is nuclear plate evidence[6] that sometimes low energy protons are emitted, indicating a nuclear excitation of about 15 Mev and that on the average 1.9 ± 0.7 low energy neutrons are emitted per meson capture in lead.[7–9] These experimental meson results are consistent with the charge exchange reaction for capture as proposed by Tiomno and Wheeler,[10] which has the form $\mu^-+P\rightarrow\mu^0+N$ where μ^0 is probably a neutrino. According to this hypothesis, most of the rest energy of the meson would be taken by the neutral particle, leaving the nucleus with about 15 Mev of excitation. The nucleus would then have lost its excitation by emitting one or two neutrons and rarely a proton. When the nuclear excitation is too low for neutron emission, low energy gamma-rays would be emitted. Tiomno and Wheeler have also shown that the excitation energy is roughly the same if the meson interacts with the whole nueleus rather than with a single proton.

Chang[2] has obtained evidence for the emission of low energy gamma-rays when a negative meson stops in lead. These may be due to Bohr orbit transitions of the meson around the nucleus. Hincks[11] has estimated the total energy of the gamma-rays emitted between 1 and 10 Mev to be near 9 Mev.

The present paper gives the results of a cloud-chamber experiment performed to investigate the nature of the low energy gamma-rays emitted when a negative meson stops in lead.

APPARATUS

The experimental apparatus, a general view of which is shown in Fig. 1 consists essentially of a cloud chamber in a magnetic field. A 1-cm lead plate is placed inside of the cloud chamber to stop and capture cosmic-ray mesons. Foils of lead are also placed in the cloud chamber so that gamma-rays from meson capture will occasionally produce pairs of Compton electrons. Thus, we would like to obtain cloud-chamber pictures which show a track stopping in the Pb plate and an electron track of the same age coming from one of the foils and tending to point back toward the meson stopping point. The cloud chamber is placed in a magnetic field so that the momentum and energy of the electrons may be determined. The energy spectrum of these electrons yields information about the gamma-rays which produce them.

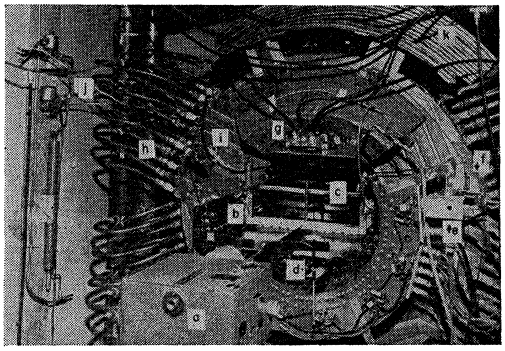

FIG. 1. Front view of the apparatus. (a) Camera; (b) mirror; (c) cloud chamber; (d) anticoincidence counters; (e) anticoincidence preamplifier; (f) tray 3 preamplifier; (g) tray 2 preamplifier; (h) water pipes for cooling coils; (i) coils; (j) compressed air valves; (k) lead shield.

* Assisted by the joint program of the U. S. Office of Naval Research and the U. S. Atomic Energy Commission.

† The experiment described in this paper was started by T. J. B. Shanley and preliminary results were obtained by him and submitted to the Department of Physics, Princeton University, in partial fulfillment of the requirements for the Doctor of Philosophy degree. G. G. Harris modified and improved the experimental arrangement and obtained the results reported in this paper. He submitted part of this material to the Department of Physics, Princeton University, in partial fulfillment of the requirements for the Doctor of Philosophy degree. It seemed advisable because of the continuity of the experiment to submit a single paper for publication.

‡ Now at the University of Bristol, Bristol, England.
§ Lieutenant Colonel now returned to duty with the United States Army and stationed at Fort Monroe, Virginia.

[1] Lattes, Muirhead, Occhialini, and Powell, Nature **159**, 694 (1947); Lattes, Occhialini, and Powell, Nature **160**, 453, 486 (1947).
[2] W. Y. Chang, Revs. Modern Phys. **21**, 166 (1949).
[3] R. D. Sard and E. J. Althaus, Phys. Rev. **73**, 1251 (1948).
[4] O. Piccioni, Phys. Rev. **74**, 1754 (1948).
[5] B. Pontecorvo, Phys. Rev. **73**, 257 (1948).
[6] E. P. George and J. Evans, Proc. Phys. Soc. (London) **A64**, 193 (1951).
[7] A. M. Conforto and R. D. Sard, Phys. Rev. **82**, 335 (1951).
[8] M. F. Crouch, Phys. Rev. **81**, 164 (1951).
[9] Groetzinger, Berger, and McClure, Phys. Rev. **81**, 969 (1951).
[10] J. Tiomno and J. A. Wheeler, Revs. Modern Phys. **21**, 153 (1949).
[11] E. P. Hincks, Phys. Rev. **81**, 313 (1951).

TABLE I. Summary of statistics from cloud-chamber photographs.

Number of pictures with particles stopping		9040
Number of pictures examined for meson curvature		2483
No curvature identified	1964	
Positive curvature	290	
Negative curvature	229	
Proportion of electrons and positrons stopping in the counter box		0.10±0.01
Positive decays from the counter box		
in an upward direction	450±20	
in a downward direction	120±30	
Positive decays in a foil	40	
Positive decay in the gas	3	
Negative mesons stopping in a foil	35	
Negative meson stopping in the gas	1	

A telescope of Geiger counters is used to control the expansion of the chamber. Two trays of Geiger counters above the cloud chamber and a third tray just above the lead plate which is inside the cloud chamber are connected in coincidence. These trays are placed so that an ionizing particle entering the cloud chamber from above will be counted by all of the trays. A fourth set of Geiger counters is placed around the bottom and sides of the cloud chamber to detect the ionizing particles which pass through the first three trays but do not stop in the chamber. The chamber is expanded when the first three trays of counters register simultaneously, but the fourth tray does not register. Six inches of lead or its equivalent in copper is placed above the cloud chamber so that most of the particles which stop in the cloud chamber will be μ-mesons.

The cloud chamber has a sensitive volume of 10 in. $\times$10 in.$\times$5 in. and is illuminated from the rear. It was originally designed for random expansions at high altitude[12] and has been modified for counter control by decreasing the expansion time. The third tray of Geiger counters, which is made from 14 counters each $\frac{1}{4}$ in. diameter$\times$7 in. sensitive length, is placed on top of the 1-cm plate and incased in a gas-tight box to provide adequate electrical shielding and to avoid turbulence. The 1-cm lead plate is a compromise in thickness. A thicker plate would stop more mesons, but the resulting gamma-ray spectrum would be altered more before leaving the plate. The lead foils are 0.0085 in. thick and are spaced 3 cm apart—two below the lead plate and one above. There is a 6-cm space above the top foil so that in favorable cases the sign of the stopping particle may be determined.

The cloud chamber was photographed by a camera which had its lens' optical axis $\frac{1}{2}$ in. to the left of the camera's horizontal front-rear axis of symmetry. This effect makes it possible both to photograph a mirror image for stereoptic purposes and to keep the optical axis of the lens parallel to the magnetic field at the chamber, thus minimizing errors on the photographed track curvature.

A magnetic field of 2000 gauss is produced by a current of approximately 180 amperes flowing through four coils. The coils act like a set of Helmholtz coils 28 in. in diameter and separated 14 in. With the cloud chamber placed in the center of this system, the magnetic field over the sensitive volume is uniform to within two percent. The coils are water-cooled with the rate of water flow controlled by a motorized valve which is regulated by a temperature sensitive element placed near the cloud chamber. All of the equipment with the exception of the electronic control circuits and the dc generator was in a temperature controlled room.

[12] R. R. Rau, Rev. Sci. Instr. **23**, 443 (1952).

MEASUREMENT, CALCULATION, AND ERRORS

All photographs of cloud-chamber expansions triggered by the coincidence-anticoincidence circuit were examined for interesting pictures. An event was selected for measurement if (1) the direct and stereo pictures showed the tracks clearly, (2) the electron track was in a favorable part of the chamber, and (3) both tracks appeared to be of the same age.

To find the curvature of an electron track, two points on the track were selected and the chord and sagitta defined by the points were measured. To compute the angle of the track with respect to the magnetic field, the depths of the two points were determined by measuring the parallax of each point from a mark on the front of the foil system. A Bausch and Lomb contour measuring projector, which enabled distances on the film to be accurately determined, was used for all measurements. The calculations of the electron energy from the curvature are made in the usual manner. However, some corrections might be mentioned. The path of a charged particle in a magnetic field being a helix, it is necessary to measure both the radius of the helix and its pitch in order to find the momentum of the particle. If a helix is photographed, the image will be in the form of a spiral with an apparent curvature different from the real curvature. Moreover, in most cases the helix is photographed inclined to its axis, thus further affecting the apparent curvature. Corrections for both effects have been applied to the curvature measurements.

One angle is also found, i.e., the angle that the electron makes with the normal to a foil as it emerges from the foil.

The main error in the determination of the electron energy is due to multiple scattering in the gas. There is an unknown energy loss in the foil in which the electron originated. Since the path length in the foil is unknown, it is assumed that each electron track was produced in the middle of the foil. Thus, the energy loss of an electron, traversing a distance equal to half a foil thickness divided by the cosine of the angle the electron makes with the foil, is added to the measured energy and to the error in energy. The errors incurred in the film measurement and in the magnetic field measurement are not large and total to about 5 percent for all tracks.

The most important error in angle determination is

caused by the multiple scattering of the electron in the foil. When the equation given in Rossi and Greisen[13] is used, it is found that the root mean square angle of multiple scattering is larger than 35° for an electron of 5 Mev traversing half of a foil thickness. This large angle of multiple scattering prohibits firm conclusions which depend upon the angular distribution of the electron tracks.

DATA

During operation of the apparatus, over 16 000 counter controlled pictures and over 6000 randomly operated pictures were taken. All of these pictures were examined once and most of them twice. Fifty-five percent of the counter controlled pictures showed a track stopping in the counter box. The remaining pictures were either blank or had tracks going through the counter box and out of the chamber. Most of the blank pictures are attributed to small showers in which a gamma-ray triggers the counters inside the cloud chamber. About 20 percent of the through tracks are due to the inefficiency of the anticoincidence counters, while the remaining through tracks are attributed to particles which stop in the matter (about 4 g cm^{-2}) between the lead plate and the anticoincidence counters. In a portion of the pictures the radius of curvature of the stopping track was recorded. The curvature of most tracks, however, cannot be judged because of distortions which were appreciable for radii of curvature of about one meter. By virtue of large curvature and minimum ionization, a portion of the stopping tracks were classified as positrons or electrons. A picture is counted as a positive meson decay if there is a positron associated with the stopping track. The statistics on curvature, etc., are given in Table I.

From Table I the positive to negative meson ratio is found to be

$$\mu^+/\mu^-=1.27\pm0.11. \quad (1)$$

This ratio, together with the proportion of stopped particles which are electrons or positrons and the total number of stopped tracks, yields the number of stopped mesons of each charge. It is found that there are $4530\pm300\mu^+$ tracks and $3580\pm300\mu^-$ tracks. Two of the the negative mesons which stopped in a foil showed a low energy electron coming from the stopping point. The electrons are probably from Compton collisions by the gamma-rays from negative meson capture and are included in the events.

None of the pictures showed heavily ionizing tracks coming from the meson stopping point. George and Evans[14] find that 8.7 percent of the negative mesons which stop in photographic plates have low energy protons (1–10 Mev) associated with them. However, our data are not inconsistent with theirs since the foil thickness is equal to the range of a 6-Mev proton.

The positive to negative meson ratio [Eq. (1)] is for particles stopping in the 1-cm lead plate after they have passed through 15-cm lead equivalent above the chamber and so includes a momentum range of about 200–220 Mev/c. This ratio is lower than the positive meson excess in the atmosphere because energetic decay positrons from stopped positive mesons may trigger the anticoincidence circuit and thus some positive mesons will be missed. As a lower estimate of the number of missed positive mesons we note from Table I that 450±20 mesons decayed in the upward direction and 120±30 decayed in the downward direction. So 330±35 decayed in the downward direction and were missed. If this is added onto the number of positive mesons, the positive to negative ratio becomes

$$\mu^+/\mu^-=1.36\pm0.12. \quad (2)$$

This result is insensitive to the percentage of protons which stopped in the counter box, since a stopping proton has too small a curvature and too large an ionization to be counted as a positive meson. The above μ^+/μ^- ratio is consistent with the results of others,[15–17] although it is not accurate enough to distinguish between a constant μ^+/μ^- ratio from 200 Mev/c to 10

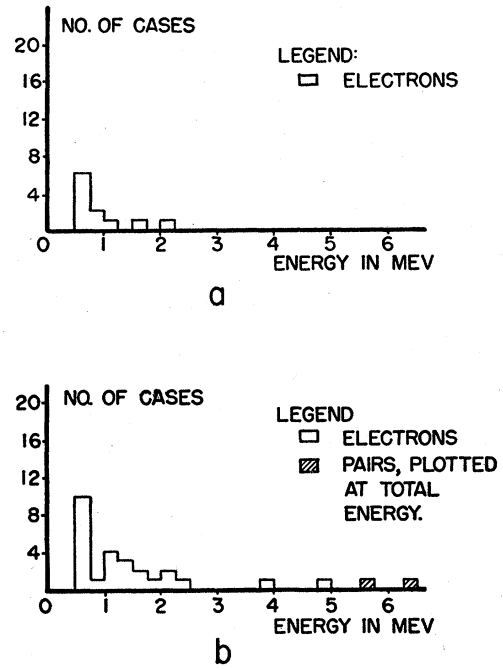

FIG. 2. (a) Histogram of events having single electrons with energy >0.5 Mev, associated with 950±100 stopped positive mesons, plotted in 0.25-Mev intervals. (b) Histogram of events having single electrons and pairs of electrons with energy >0.5 Mev, associated with 750±80 stopped negative mesons, plotted in 0.25-Mev intervals.

[13] B. Rossi and K. Greisen, Revs. Modern Phys. **13**, 240 (1941).
[14] E. P. George and J. Evans, Proc. Phys. Soc. (London) **A64**, 193 (1951).
[15] R. B. Brode, Phys. Rev. **78**, 92 (1950).
[16] Glaser, Hamermesch, and Safanov, Phys. Rev. **80**, 625 (1950).
[17] B. G. Owen and J. Wilson, Proc. Phys. Soc. (London) **A62**, 601 (1949).

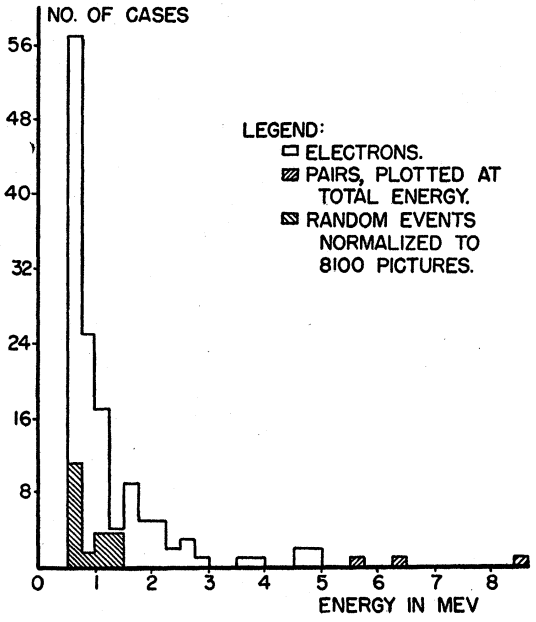

FIG. 3. Histogram of all events having single electrons and pairs of electrons with energy >0.5 Mev associated with stopped mesons, plotted in 0.25-Mev intervals.

Bev/c and a ratio which increases with decreasing momentum.

Figure 2 shows histograms of electron tracks with energy greater than 0.5 Mev associated with stopping meson tracks of different sign. A careful survey of all events was made to determine the charge of the stopping particle. Only cases which showed a clear curvature were identified with a sign. From the information in Table I we can estimate the total number of identifiable positive mesons. The events associated with a positive stopping track are attributed to this number of mesons. A similar number was estimated for the electrons associated with a negative stopping track. Figure 3 shows the histogram of the electron tracks of the correct age found in the random expansions normalized to the number of stopped mesons together with a histogram of all electron tracks associated with stopping mesons.

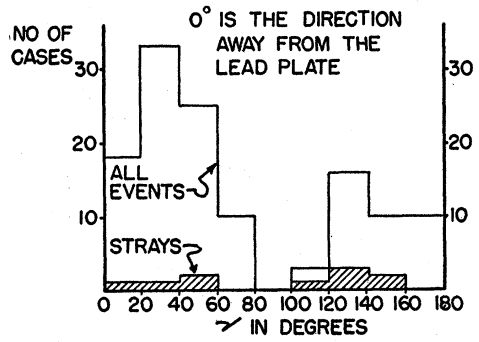

FIG. 4. Histogram showing the distribution of γ, the angle between the vertical and the electron track.

A histogram of the angular distribution with respect to the vertical direction is shown in Fig. 4. In spite of the multiple scattering, it is evident that there is a rough angular correlation. In Fig. 4 the zero angle is taken as away from the lead plate, i.e., upwards above the plate and downwards below the plate. The greater number of events have $\gamma<90°$, which supports the hypothesis that the parent photons come from the lead plate.

Three cases of pairs associated with a stopping meson were found and are listed in Table II. In Fig. 5 a meson stops in the first foil and a pair comes from the foil. The electron track could be caused by a positron from the lead plate which scatters in the first foil and then in the lead plate, but the picture is taken as a pair because of the small chance of a meson stopping in a foil with a scattered positron which is space and time coincident. The other two pictures attributed to pairs show two tracks of different energy coming from the same point. The more energetic track tends to point back at the stopping meson. These two pictures were selected as pairs because of this angular correlation and because, if one particle is assumed to produce the event by scattering, the particle would suffer an improbable energy loss.

There are too few pairs to draw any conclusions. Event A is consistent with a 4.5-Mev Bohr orbit transition but may also be due to a nuclear gamma-ray. The same may be said for event C. Event B has higher energy than might be expected from negative meson capture, and, since the charge of the stopping meson is unknown, it could be attributed to bremsstrahlung from a decay positron.

ANALYSIS OF THE DATA

Given an electron spectrum, our problem is to find the spectrum of parent gamma-rays which produce the electrons by the Compton and photoelectric effects. Now, for a particular gamma-ray energy the photoelectric effect gives a unique electron energy. However, monoenergetic gamma-rays produce a continuous spectrum of Compton electron energies. It is difficult, therefore, to determine a unique gamma-ray spectrum from an electron spectrum in a direct manner. Rather, our approach will be to assume a gamma-ray spectrum, calculate the resulting electron distribution, and see if it is consistent with the data.

We wish to test the hypothesis that when a negative meson is captured by a lead nucleus, gamma-rays are emitted both from Bohr orbit transitions of the meson around the nucleus and from the nucleus after meson capture. We, therefore, calculate the expected electron spectra from Bohr orbit and nuclear gamma-rays. Since the gamma-rays originate in the lead plate, some will be absorbed. A portion of these will give secondary gamma-rays of lower energy which will be added to the original spectrum. Of the number that leave the lead

plate, only a small fraction will produce electrons in the foils.

Our data show that there are a number of electron tracks associated with stopping positive mesons. These electrons are attributed to bremsstrahlung gamma-rays from decay positrons (about 80 percent of these positrons do not get out of the lead plate) and to radiation from positrons which are annihilated in flight. The annihilation spectrum, however, is similar in shape to the electron spectrum due to bremsstrahlung, but about one-tenth the magnitude, so only bremsstrahlung is considered. A spectrum due to stray gamma-rays is also estimated.

The photoelectric effect, Compton effect, and pair production are important in the energy range from 1–10 Mev. In particular, gamma-rays produced in the lead plate will be absorbed by all three processes. However, we assume that only gamma-rays which are absorbed by the Compton process will produce additional gamma-rays.

The differential radiation probability for electrons of 1 to 50 Mev is difficult to estimate accurately. Rossi and Greisen[13] have calculated the differential radiation

TABLE II. Energy of observed pairs.

	Energy in Mev	Sign of stopping track	γ-ray energy in Mev
A	$e^+=3.8\pm0.8$ $e^-=0.8\pm0.5$	negative	5.6 ± 1.2
B	$e^+=0.4\pm0.3$ $e^-=7.0\pm1.1$	unknown	8.4 ± 1.4
C[a]	$e^+=2.4\pm0.5$ $e^-=2.9\pm0.7$	negative	6.4 ± 1

[a] In event *C* a negative meson stops in a foil and the pair starts from the same point.

probability per radiation length $\rho(v)dv$ for an electron of 10 Mev and found it to be approximated by the formula

$$\rho(v)dv=(4/3)(1-v)dv/v, \quad (3)$$

where v is defined as the ratio W/E of the energy of the secondary photon to the total energy of the electron. The energy loss by collisions from 1 to 50 Mev is well approximated by

$$(dE/dx)_{\text{coll}}=-1.5 \text{ Mev/g cm}^2. \quad (4)$$

From these assumptions the expected electron spectrum ejected from the foils by bremsstrahlung gamma-rays is calculated and is shown in Fig. 6. This is the number expected per Mev per positron, which loses all its energy in the lead, and has to be multiplied by the number of positive mesons stopping in the lead plate and by the fraction of absorbed positrons per stopped positive meson. We can check this spectrum by comparing it with the data due to stopped positive mesons, which represent the electrons from 950 ± 100 mesons. The total number of electrons from 0.75–10 Mev expected for 950 mesons is found to be 10.8 electrons.

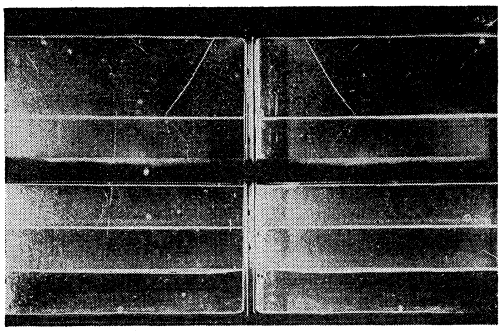

FIG. 5. A heavily ionizing negative particle stops in the first lead foil. An electron-positron pair emerge from the stopping point and enter the counter box. The energy of the photon which produced the pair is calculated to be 6.4 ± 1 Mev (event *C* in Table II).

The actual number of electrons observed was 5 ± 2. In order to apply a correction for the positive mesons, we assume that the shape of the spectrum is correct and that only its absolute magnitude is in error. If η is a normalization factor and σ is the efficiency for detecting electrons, then $\eta\sigma=0.46$. Since the efficiency as determined by the spectrum from negative mesons is close to 1, η must be close to 0.46. There are two factors which help to explain the small η. (1) High energy decay positrons tend to escape from the plate so that the spectrum absorbed in the plate has a low average energy. (2) If a decay positron is traveling in a direction such that a bremsstrahlung gamma-ray would pass through a foil, it has a larger than average chance of escaping from the plate and so would not be as likely to produce bremsstrahlung gamma-rays.

It is necessary to know three things about an excited nucleus in order to calculate the gamma-ray spectrum. None of these factors is known precisely. The first is the nuclear excitation energy. After a lead nucleus captures a negative meson, it will have about 15 Mev of excitation. According to Bethe,[18] in heavy elements neutron emission predominates over photon emission when the nuclear excitation is greater than the neutron dissociation energy by only a few kev. Since the disso-

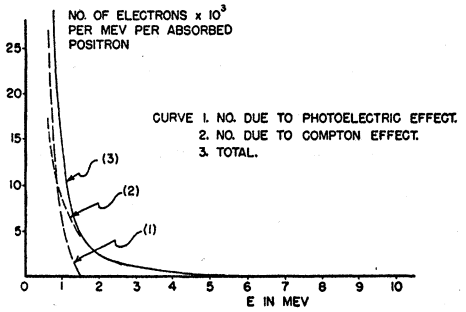

FIG. 6. Number of electrons of energy E produced in the foils by bremsstrahlung from a 37-Mev positron absorbed in the lead plate.

[18] H. Bethe, Revs. Modern Phys. **9**, 160 (1937).

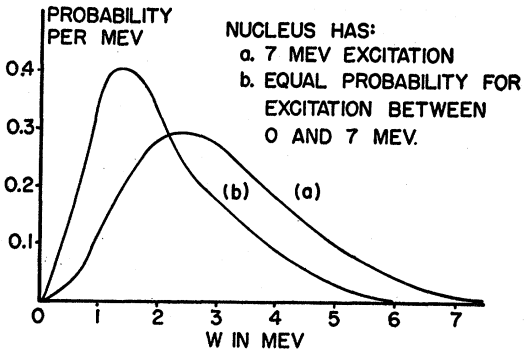

FIG. 7. First photon spectra from a heavy nucleus. Dipole radiation and energy level density $\sim\exp(1.2E)$ are assumed.

ciation energy for a lead nucleus is around 7 Mev, the nucleus will have an excitation ranging from 0 to 7 Mev after particle emission. The probability that it will have a particular energy is unknown. The second unknown factor is the type of radiation, i.e., dipole or quadrupole. The third is the energy level density $D(E)$ of the excited lead nucleus.

For simplicity in calculation, the following two sets of assumptions are made:[19] I dipole radiation with $D(E)\sim e^{1.2E}$ and all nuclei start with 7-Mev excitation; II dipole radiation with $D(E)\sim e^{1.2E}$ and the nuclei have any energy between 0 and 7 Mev with equal probability. The spectra for these models are calculated, assuming that each nucleus emits two photons. The first photon spectrum for each of these models is shown in Fig. 7.

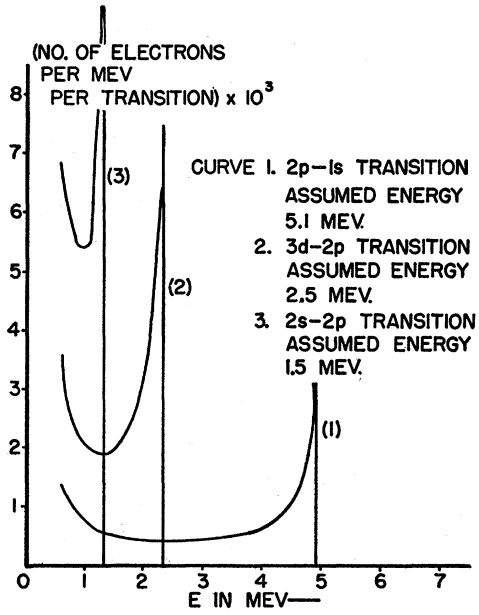

FIG. 8. Expected electron spectra from Bohr orbit transitions.

[19] There is some evidence for a level density $D(E)\sim e^{1.2E}$ for lead for the energy range 6–10 Mev from neutron emission experiments [see P. C. Gugelot, Phys. Rev. 81, 51 (1951)].

Theory[10] predicts that when a negative meson is captured by a nucleus, there should be energetic Bohr orbit transitions. For lead there should be a $2p-1s$ transition of about 4.5 Mev for nearly every meson capture and a high probability of a $3d-2p$ transition of around 2.5 Mev or a $2s-2p$ transition of around 1.5 Mev. Because of the number of electrons between 4.5 and 5 Mev, a $2p-1s$ transition of 5.1 Mev is assumed and spectra calculated. However, because all the events between 3.5 Mev and 5.5 Mev are grouped together, the data is insensitive to the exact energy of the $2p-1s$ transition. Electron spectra are also calculated for 2.5 and 1.5 Mev gamma-rays. One of the calculated curves is shown in Fig. 8.

Our data indicates that the stray background electrons are not negligible. So we have assumed a spectrum of gamma-rays proportional to $1/W$, where W is the gamma-ray energy. This spectrum seems reasonable in view of the $1/W$ dependence of bremsstrahlung and also the fact that any Compton collisions will tend to build up the low energy portion of the spectrum rather than the high energy region. The calculated electron spectrum is normalized to the observed number of background events.

Only electrons with energy greater than 0.75 Mev are considered in the statistical analysis because both the errors in measurement and in calculation increase rapidly for lower energies. In order to test the consistency of various assumed photon spectra, the data is divided into groups. The various expected electron spectra are summed up over the same groups and the sums are listed in Table III. The bremsstrahlung spectrum has been multiplied by $\eta=0.46$. The background spectrum has been normalized to 9.6 electrons. Since in 5860 pictures there were 7 random events, in 8100 pictures, therefore, there should be 9.6 ± 3 events.

For the most general type of fit, suppose (1) that the $2p-1s$ transition occurs with every negative meson capture, (2) that the $2s-2p$ transition occurs a fraction f_1 of the time, (3) that the $3d-2p$ transition occurs a fraction f_2 of the time, and (4) that the nuclear photon spectra have a multiplying factor m. Let the efficiency for detecting an electron be σ.

If we assume that the meson reaches the $2p$ state either from the $2s$ or $3d$ state ($f_1+f_2=1$), then the condition that the total number of expected electrons should equal the observed number of electrons yields $m+0.084f_2=(1.92/\sigma)-1.01$ for nuclear model I. The most important variables are m and σ. If the efficiency is low, then m is large, which means a lot of energy in nuclear gamma-rays. Since we would expect $m<1.5$, we shall assume that the efficiency is unity.

Another condition is imposed by finding a weighted least square fit to the data which determines f_1, f_2, and m. The values found for both nuclear model I and model II are listed in Table IV.

The chi-square test is used as a statistical test of consistency. The quantity $\chi^2=\sum_i(x_i-n_i)^2/n_i$ is com-

TABLE III. Number of electrons expected and observed.

Assumed spectra		Group 1 Energy range in Mev 0.75–1	2 1–1.25	3 1.25–1.5	4 1.5–2	5 2–2.5	6 2.5–3.5	7 3.5–4.5	8 4.5–5.5	Total 0.75–10.0
Bremsstrahlung	a_i[a]	9.00	4.63	2.60	2.73	1.57	1.97	0.84	0.31	23.8
Stray background	b_i	2.41	1.41	0.93	1.14	0.75	1.06	0.58	0.38	9.65
$2p-1s$ (5.1)[b]	c_i	0.81	0.58	0.46	0.79	0.75	1.62	2.57	2.31	9.89
$2s-2p$ (1.5)	d_i	5.19	6.65	1.29						13.10
$3d-2p$ (2.5)	g_i	2.20	1.76	1.74	4.72	4.62				15.0
Nuclear mod. I	j_i	4.86	3.72	2.79	3.65	2.72	3.54	1.14	0.28	22.7
Nuclear mod. II	j_i^1	7.15	4.58	2.72	2.07	0.93	1.00	0.32	0.07	18.8
Data[c]	x_i	25	17	4	14	7	4	2	4	77

[a] a_i, b_i, etc., are the number of electrons expected in this experiment in each group i.
[b] The number in parentheses refer to the assumed transition energy in Mev.
[c] The actual number of electrons observed in each group.

puted, where x_i is the observed number of electrons in a group, n_i is the predicted number of electrons, and the sum is over all the groups. The function $F(\chi^2)$ gives the probability of finding in another set of data a χ^2 which is larger than the given χ^2, providing that the data is really from the assumed parent distribution. For a given χ^2 the values of $F(\chi^2)$ depend on the number of degrees of freedom in the data. In order that the values of $F(\chi^2)$ will be comparable, the same grouping is used for each assumed spectra. The results of these tests are listed in Table IV.

For the chi-square test to be reliable, the number of degrees of freedom N^1 and the expected value n_i of any group should not be too small. One criterion is that N^1 should be 4 or greater and that all n_i should be 5 or greater. In the tests listed in Table IV all N^1 are 4 or greater, but sometimes the n_i are less than 5. However, in all cases where an n_i is less than 5, a regrouping does not lead to substantially different results, so the original groupings are listed.

The total energy per μ^- capture emitted in gamma-rays from 0.75 to 7 Mev has been computed for the different spectra and is listed in Table IV. For this purpose the $2p-1s$ transition was assumed to be 5.1 Mev.

DISCUSSION AND CONCLUSIONS

By studying the energies and directions of the electrons associated with μ-mesons which stop in the lead plate of the cloud chamber, we conclude that these electrons are produced by photons with energy between 0.75 and 7 Mev which are also associated with the stopping mesons. By noting the sign of some of the stopping μ-mesons, we are able to confirm the existence of photons associated with the capture of negative μ-mesons in lead. More direct evidence for the existence of photons is given by two cloud-chamber pictures which show a negative meson stopping in an 0.0085-in. lead foil and an electron emerging from the same spot. Another picture shows a negative meson which stops in a foil with a pair coming from the stopping point.

Of the two spectra which were fitted to the data by the method of least squares, the spectrum using nuclear model II is the more consistent. The total energy emitted for this spectrum is 10.6 Mev which is consistent with the estimate of Hincks.[11] The fact that the nuclear gamma-ray spectrum which has more low energy gamma-rays fits the data best is a justification for the use of dipole radiation in the calculations, since quadrupole radiation would give a higher average energy.

When only nuclear photons are assumed, $F(\chi^2)\sim 0.08$ for both nuclear models. Not only are these distributions unlikely, but to account for the data the nucleus has to emit a total energy of 10.4 Mev for nuclear model I, where the nucleus has 7 Mev excitations, or a total energy of 7.2 Mev for nuclear model II, where the nucleus has an average energy of 3.5 Mev. These total energies are inconsistent with the assumed spectra. Again, when only Bohr orbit transitions are considered, $F(\chi^2)\sim 0.10$ which not only indicates a poor fit, but also means that the total energy emitted (13.2 Mev) is inconsistent with theory. From these two types of assumed spectra, we conclude that neither nuclear

TABLE IV. Summary of fits to the data.[a]

Assumed spectra	$\Sigma n_i=\Sigma x_i$	E_t	χ^2	N^1	$F(\chi^2)$
Bohr orbit transition and					
Nuc. mod. I	($m=0.87$, $f_2=0.45$)	11.7	7.59	4	0.10
Nuc. mod. II	($m=1.03$, $f_2=0.75$)	10.6	4.89	4	0.30
Nuclear gamma-rays alone:					
Nuc. Mod. I	$m=1.92$	10.4	9.37	5	0.10
Nuc. Mod. II	$m=2.32$	7.2	11.37	5	0.05
Bohr orbit transitons alone:	($M=1.84$, $f_2=0.56$)	13.2	7.99	4	0.10
No $2p-1s$ transition					
Nuc. mod. I	($m=1.30$, $f_2=0.46$)	9.0	7.01	4	0.13
Nuc. mod. II	($m=1.53$, $f_2=0.91$)	7.1	5.91	4	0.20
All stray background	$M=7.98$	···	11.57	5	0.04
All bremsstrahlung	$M=3.24$	10.0	9.20	5	0.10
		($2p-1s=5.1$ Mev)			

[a] $\Sigma n_i=\Sigma x_i$ is the condition that the total number of predicted electrons should equal the total number of observed electrons. To make this equation hold the following multiplying factors are used: f_2 is the coefficient for the $3d-2p$ transition spectra. f_1 is the coefficient for the $2s-2p$ transition spectra, which is found from the equation $f_1+f_2=1$. m is the multiplicity coefficient for the nuclear spectra. M is the normalizing factor when applied to the whole spectrum. The values of m and f_2 listed for the first two spectra are determined with the additional condition that the assumed spectra make a weighted least square fit to the data. E_t is the total energy in Mev per μ^- meson capture in lead emitted by photons between 0.75 and 7 Mev. χ^2 is defined by the sum $\chi^2=\Sigma(n_i-x_i)^2/n_i$. N^1 is the number of degrees of freedom of the statistical sample for purposes of the chi-square test. $F(\chi^2)$ is a statistical measure of consistency. It gives the probability of finding another χ^2 which is larger than the given χ^2 if the experimental data really comes from the assumed source.

gamma-rays alone nor Bohr orbit transitions alone will explain the observed spectra. This conclusion is based on the assumption that the residual thallium nuclei are not unstable with a lifetime short enough to be within the resolving time of the cloud chamber ($\sim$0.05 second). It is unlikely that there are such short lifetimes among the residual nuclei. If we take the experimental evidence on the emission of neutrons and protons from meson capture, then from a Segrè chart the most unfavorable lifetime is about three minutes.

Nothing definite can be said about the existence of a $2p-1s$ Bohr orbit transition. For if the $2p-1s$ transition is emitted from the assumed spectra the spectra which remain are consistent with the data. The data is consistent with the assumed spectra being totally due to bremsstrahlung photons from positrons and stray background photons. It is extremely unlikely, however, that the data could be accounted for by stray background photons alone, and the data could not be accounted for by bremsstrahlung photons alone because of the large numbers of electrons associated with negative mesons.

We wish to thank Professor R. Ronald Rau for encouragement and helpful discussions. We are grateful to Professor George T. Reynolds and Dr. J. W. Keuffel and Dr. Georgio Salvini for assistance.

PHYSICAL REVIEW VOLUME 89, NUMBER 5 MARCH 1, 1953

The Acousto-Electric Effect*

R. H. PARMENTER
Massachusetts Institute of Technology, Cambridge, Massachusetts
(Received November 25, 1952)

A new effect, the acousto-electric effect, is predicted on the basis of theoretical calculations. This effect deals with the generation of an electric current by a traveling longitudinal acoustic wave. The time-average of the generated current is found to depend on the sound power but not on the frequency of the acoustic wave. Illustrative calculations on a metal (sodium) and a semiconductor (n-type germanium) indicate that the effect should be experimentally measurable. An interesting analogy with the thermoelectric effect is pointed out.

I. INTRODUCTION

IN this paper we discuss the effect on the conduction electrons of a crystal resulting from a single traveling longitudinal acoustic wave in the crystal. It is not difficult to see qualitatively how the electrons will be affected when the amplitude of the acoustic wave is small. The presence of a sinusoidal traveling acoustic wave gives rise to a sinusoidal electric field, this field traveling through the crystal with the same velocity as that of the acoustic wave. Consider the component of velocity of a conduction electron parallel to the velocity of the acoustic wave. For most of the conduction electrons, this component of velocity will be much larger in magnitude than the speed of the acoustic wave, so that these electrons are "out of phase" with respect to the traveling electric field. Thus, the time average of this field over their trajectories is zero, and these electrons are essentially unaffected by the presence of the acoustic wave. There are a few electrons, however, having components of velocity parallel to the wave which are comparable to the speed of the wave. These electrons are capable of being trapped by the moving electric field so that their time-averaged velocity in the direction of the field is exactly that of the field. Among these electrons, those having a maximum energy will be found to give rise to a net electric current. In a metal, these electrons are at the Fermi level. In an n-type semiconductor, these electrons are in the conduction band. Such a generation of an electric current by a traveling acoustic wave may be called the acousto-electric effect. It is interesting that the qualitative explanation of this effect which has just been given is analogous to the qualitative explanation of the operation of a linear accelerator.[1]

Let us consider a single traveling longitudinal acoustic wave moving along a long uniform rod of material, the ends of the rod being electrically insulated. The traveling acoustic wave could be induced by driving one end of the rod with a vibrator while matching the other end to the proper acoustic impedance to insure no reflection of the wave at the termination. The ends of the rod being electrically insulated, the acoustic wave would drag conduction electrons to one end of the rod, creating a deficiency of electrons at the other end. The resultant electric field along the rod will generate a conventional electric current which exactly cancels the current associated with the acousto-electric effect. The acousto-electric effect, therefore, may be measured by determining the electric potential difference between the two ends of the rod. An interesting comparison pointed out to the writer[2] is the striking analogy between this

* This work was supported by the U. S. Office of Naval Research.

[1] J. C. Slater, Revs. Modern Phys. **20**, 473 (1948). See especially p. 483.
[2] H. Brooks, private communication.

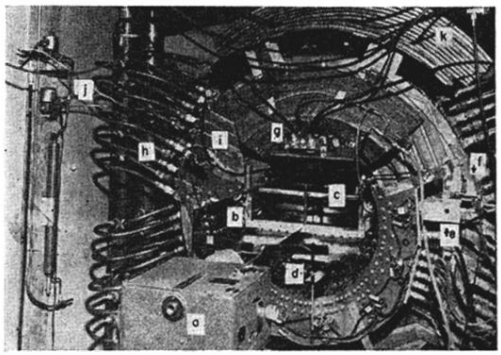

FIG. 1. Front view of the apparatus. (a) Camera; (b) mirror; (c) cloud chamber; (d) anticoincidence counters; (e) anticoincidence preamplifier; (f) tray 3 preamplifier; (g) tray 2 preamplifier; (h) water pipes for cooling coils; (i) coils; (j) compressed air valves; (k) lead shield.

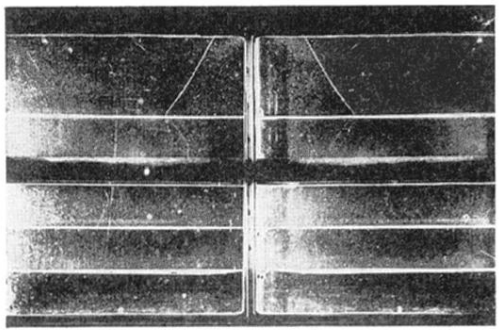

FIG. 5. A heavily ionizing negative particle stops in the first lead foil. An electron-positron pair emerge from the stopping point and enter the counter box. The energy of the photon which produced the pair is calculated to be 6.4 ± 1 Mev (event *C* in Table II).